Transcription factor regulation of eQTL activity across individuals and tissues

Elise D. Flynn[1,2], Athena L. Tsu[2,3], Silva Kasela[1,2], Sarah Kim-Hellmuth[1,2,4], Francois Aguet[5], Kristin G. Ardlie[5], Harmen J. Bussemaker[1,6], Pejman Mohammadi[7,8,#], Tuuli Lappalainen[1,2,9,#]

[1] Department of Systems Biology, Columbia University, New York, NY, USA

[2] New York Genome Center, New York, NY, USA

[3] Department of Biomedical Engineering, Columbia University, New York, NY, USA

[4] Department of Pediatrics, Dr. von Hauner Children's Hospital, University Hospital, LMU Munich, Munich, Germany

[5] The Broad Institute of MIT and Harvard, Cambridge, MA, USA

[6] Department of Biological Sciences, Columbia University, New York, NY, USA

[7] Department of Integrative Structural and Computational Biology, The Scripps Research Institute, La Jolla, CA, USA

[8] Scripps Translational Science Institute, The Scripps Research Institute, La Jolla, CA, USA

[9] KTH Royal Institute of Technology, Stockholm, Sweden

[#] Corresponding authors: pejman@scripps.edu, tlappalainen@nygenome.org

Abstract

Tens of thousands of genetic variants associated with gene expression (*cis*-eQTLs) have been discovered in the human population. These eQTLs are active in various tissues and contexts, but the molecular mechanisms of eQTL variability are poorly understood, hindering our understanding of genetic regulation across biological contexts. Since many eQTLs are believed to act by altering transcription factor (TF) binding affinity, we hypothesized that analyzing eQTL effect size as a function of TF level may allow discovery of mechanisms of eQTL variability. Using GTEx Consortium eQTL data from 49 tissues, we analyzed the interaction between eQTL effect size and TF level across tissues and across individuals within specific tissues and generated a list of 6,262 TF-eQTL interactions across 1,598 genes that are supported by at least two lines of evidence. These TF-eQTLs were enriched for various TF binding measures, supporting with orthogonal evidence that these eQTLs are regulated by the implicated TFs. We also found that our TF-eQTLs tend to overlap genes with gene-by-environment regulatory effects and to colocalize with GWAS loci, implying that our approach can help to elucidate mechanisms of context-specificity and trait associations. Finally, we highlight an interesting example of IKZF1 TF regulation of an *APBB1IP* gene eQTL that colocalizes with a GWAS signal for blood cell traits. Together, our findings provide candidate TF mechanisms for a large number of eQTLs and offer a generalizable approach for researchers to discover TF regulators of genetic variant effects in additional QTL datasets.

Author Summary

Gene expression is regulated by local genomic sequence and can be affected by genetic variants. In the human population, tens of thousands of *cis*-regulatory variants have been discovered that are associated with altered gene expression across tissues, cell types, or environmental conditions. Understanding the molecular mechanisms of how these small changes in the genome sequence affect genome function would offer insight to the genetic regulatory code and how gene expression is controlled

across tissues and environments. Current research efforts suggest that many regulatory variants' effects on gene expression are mediated by them altering the binding of transcription factors, which are proteins that bind to DNA to regulate gene expression. Here, we exploit the natural variation of TF activity among 49 tissues and between 838 individuals to elucidate which TFs regulate which regulatory variants. We find 6,262 TF-eQTL interactions across 1,598 genes that are supported by at least two lines of evidence. We validate these interactions using functional genomic and experimental approaches, and we find indication that they may pinpoint mechanisms of environment-specific genetic regulatory effects and genetic variants associated to diseases and traits.

Introduction

Gene expression is regulated by local genomic sequence and can be affected by genetic variants. In the human population, tens of thousands of *cis*-regulatory variants have been discovered by expression quantitative trait locus (eQTL) mapping that associates genetic variation to gene expression levels. These variants are enriched to fall in *cis*-regulatory elements and transcription factor binding sites [1–3], implying that many eQTLs act via allelic difference in transcription factor affinity. However, specific mechanisms of individual eQTL effects and their variation across tissues or other contexts remain elusive. Understanding eQTL mechanisms, as well as the contexts in which they are active, can shed light on the regulatory code of the genome and how genetic variation perturbs this regulation.

Multiple efforts have sought to catalog eQTL effects across different contexts. The GTEx Consortium profiled gene expression in 49 tissues across 838 donors and discovered eQTLs for 1,260-18,795 genes per tissue [4,5]. Approximately a third of these eQTLs were estimated to be active in all or almost all tissues, while a fifth were estimated to be active in five or fewer tissues. Further work using computational cell type deconvolution has discovered approximately three thousand GTEx eQTLs whose effects are likely cell-type-specific [6]. Additional context-specific eQTL effects have been assayed in a

47 variety of settings, including during immune stimulation [7,8], cell stress [9,10], cell differentiation [11],
48 and drug or nutrient exposure [12–14].

49 However, few studies have been conducted to investigate what causes eQTL context specificity,
50 i.e., why eQTLs are differentially active across contexts. Some of this variation is of course explained by
51 gene expression: genes that are not expressed will not have a measurable eQTL. However, multiple
52 studies have found that the link between gene expression and eQTL effect is not straightforward,
53 observing both increasing and decreasing allelic effects with increasing gene expression [5,15]. When
54 investigating the tissue variability of GTEx eQTLs, we discovered that ~4% of eQTLs show increasing effects
55 with increasing gene expression across tissues, and ~4% show decreasing effects [5]. These findings show
56 that the context variability of eQTL effects cannot be explained by gene expression alone and must depend
57 on other features, such as chromatin accessibility, enhancer looping, or variable levels of transcription
58 factor binding.

59 Determining eQTLs' mechanisms of action is challenging. The first obstacle lies in identifying the
60 causal variant(s) of a locus from the typically numerous associated variants in high linkage disequilibrium
61 (LD). Putatively functional variants can be pinpointed by statistical fine-mapping approaches,
62 complemented with genomic annotations such as regions of open chromatin, TF binding sites predicted
63 by motifs, or allele-specific binding of TF ChIP-seq data [5,16–19]. However, these annotations suffer from
64 both low specificity and low sensitivity. In terms of specificity, a large percentage of variants in the genome
65 overlap some functional annotation; for instance, Gaffney et al found that 40% of SNPs in eQTLs
66 overlapped a DNAse I hypersensitive site or histone-modified region [2]. In terms of sensitivity, functional
67 data may be missing for the context in which the eQTL is active, and especially the highly informative
68 allelic binding data are relatively sparse [20–22]. While experimental assays that directly measure
69 regulatory effects of variants are increasing in scale, they may miss *in vivo* interactions or chromatin-

70 specific regulation [23], and intensive experimental approaches to directly profile the effects and
71 mechanisms of genetic variants in an eQTL [24–27] are difficult to conduct in a high-throughput manner.

72 One thing made clear by functional annotation data is that both eQTLs and chromatin-QTLs are
73 enriched in known TF binding sites [2,4,28]. Given that TFs are one of the few sequence-specific
74 interactors with the genome, it follows that noncoding eQTLs may exert their effects by altering TF
75 binding, which would then affect chromatin accessibility, histone modifications, and gene expression.
76 Adding to the hypothesis that TF binding may control eQTL variability, many cross-tissue eQTLs are
77 enriched in TF binding sites for TFs with broad activity, while tissue-specific eQTLs are enriched for those
78 relevant to their observed tissue [29]. By determining which TF's binding is being altered by an eQTL, we
79 would be able to identify its mechanism of action, as well as understand what could be regulating the
80 eQTL's context variability.

81 In this study, we set out to discover TF regulators of eQTLs by identifying eQTL effects that
82 correlate with TF levels across or within tissues, using primarily GTEx data. We use the natural variation
83 of TF levels between tissues, individuals, and conditions to elucidate mechanisms of action of eQTL
84 regulatory variants and understand the context specificity of eQTL effects. We hypothesize that a portion
85 of the observed context variability of an eQTL may be explained by the level of the TFs that bind to the
86 eQTL to regulate gene expression [Fig. 1A-C]. In the simplest form of the model, an allele may increase
87 the affinity of an activating TF in a *cis*-regulatory site, which would lead to higher gene expression of that
88 allele [Fig. 1A]. However, at low TF levels, the TF would not bind to either allele, resulting in the same low
89 level of background gene expression from each allele. Conversely, at very high TF levels of saturated
90 binding, even the lower affinity allele could bind the TF, and both alleles would have equal gene
91 expression. This would translate to increasing and then decreasing eQTL effects as TF levels increase [Fig.
92 1C]. Other models are explored in the supplement [SFig. 1].

93 Our approach links variation in TF levels to variation in eQTL effect size and requires no additional
94 datatypes to be captured, using the same genetic and gene expression data that are used for eQTL
95 discovery. It offers a novel approach to understanding regulatory variant context specificity that can refine
96 and complement existing approaches based on statistical fine-mapping and functional genomic
97 experiments. Applying it to GTEx data, we find thousands of interactions between TF levels and eQTL
98 effects both across tissues and within tissues which represent potential TF regulators of eQTL effects, and
99 we validate these data using numerous approaches and datasets. Finally, we highlight an example of an
100 IKZF1-regulated eQTL that colocalizes with multiple GWAS blood traits, evidencing how this TF-based
101 model can be used to unravel effects on human health and disease.

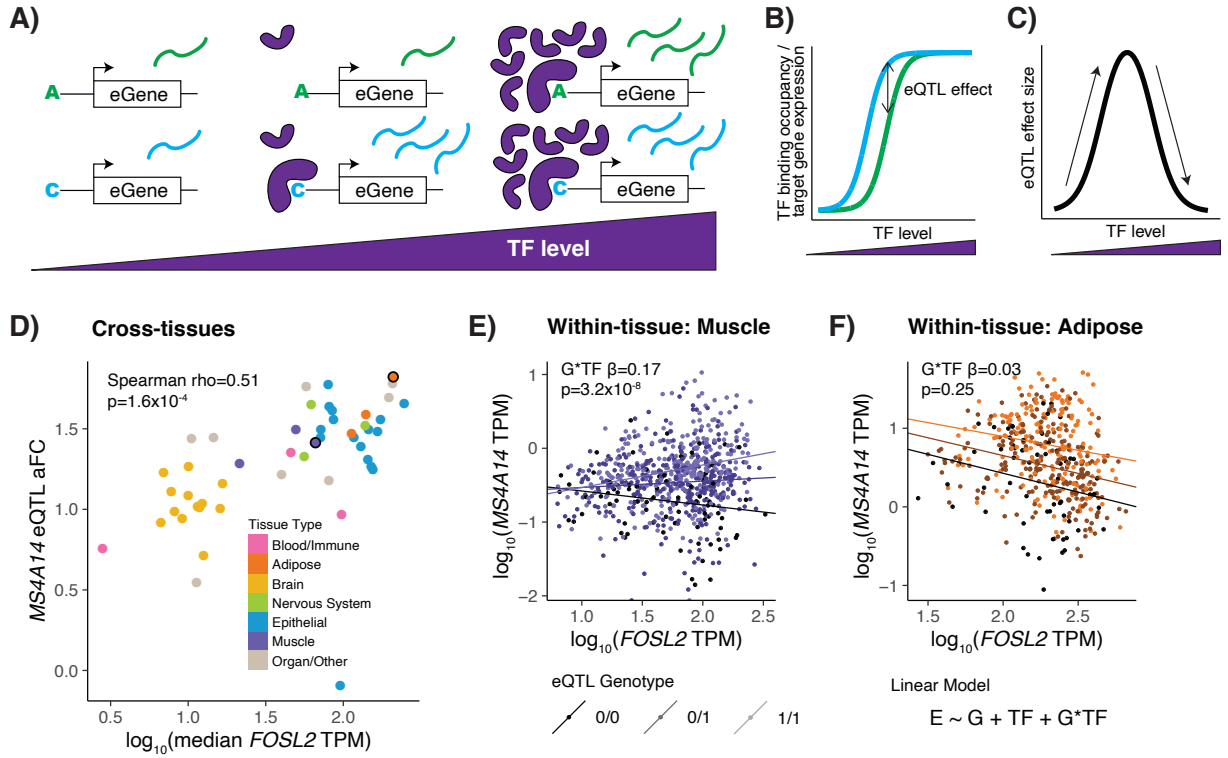

102

103 ***Figure 1. TF model of eQTL effects. A)*** *TF binding to an eQTL variant with different allelic TF affinities is depicted at low, medium,*
104 *and high TF levels.* ***B)*** *TF binding occupancy, resulting in target gene expression, for the two eQTL alleles across TF levels.* ***C)***
105 *Difference in expression of alleles or eQTL effect size, quantified as* $\log_2$ *allelic fold change, across TF levels. Our applied models*
106 *only examine monotonic effects, which can be imagined as different sides of the hill.* ***D)*** *Tissues are plotted by eQTL effect size vs.*

median TF expression for an example MS4A14 *eQTL and the FOSL2 TF. Cross-tissue TF-eQTL interactions are discovered by a Spearman correlation of these two measures, or with TF protein levels for the protein-based analysis. Two tissues circled in black are highlighted in the following panels.* ***E)*** & ***F)*** *Individuals are plotted by eGene expression vs. TF expression in Skeletal Muscle (E) or Adipose Visceral (F) tissue and are shaded by the genotype of the eQTL variant. Within-tissue TF-eQTL interactions are discovered using a multiple linear regression interaction model of normalized eGene expression by TF level, genotype, and TF level by genotype. Linear regression lines are plotted separately for each genotype, with corresponding G*TF interaction beta and p-value displayed on the chart. In Muscle, an eQTL is present, observable as a difference between the genotypes, and the difference gets larger as TF expression is higher, suggesting an interaction between TF level and eQTL effect. In Adipose, an eQTL is present, observable as a difference between the genotypes, but that difference does not appear to correlate with TF level.*

Results

Selection of putative regulatory variants

For the bulk of our analysis, we used the GTEx v8 dataset, including whole genome sequencing for 838 individuals and RNA sequencing from 73-706 samples across 49 tissues [STable 1]. We focused our analysis on common variants (>5% MAF) that have prior evidence of affecting gene expression and being regulated by a TF [Table 1]. We used Caviar fine-mapping of GTEx eQTLs in 49 tissues to select variants that fell into a 95% credible set in at least one tissue [5,30]. We also required evidence that a TF binds in the vicinity of the variant. We focused our analysis on 169 TFs with both ENCODE ChIP-seq and HOCOMOCO motif information and included variants that overlapped at least one ChIP-seq peak and matched at least one motif for these TFs.

Filtering based on an intersection of these fine-mapping and functional annotations left us with 473,057 variants that corresponded to 1,032,124 eQTLs across 32,151 genes. Each variant was associated with a median of two genes, and each gene was associated with a median of 28 variants across tissues [SFig. 2]. Next, we used cross-individual and cross-tissue analyses to discover which of this large number of candidate variants had additional evidence of TF mechanisms underlying their eQTL effects.

131 ***Table 1. GTEx variant annotations.***

Dataset	>5% MAF GTEx variants	
	Count	Percent
All	6,539,590	-
Caviar fine-mapped set	2,867,556	44%
ENCODE TF ChIP-seq peak	1,425,613	22%
HOCOMOCO TF motif	3,716,312	57%
Intersection	473,057	7%

132

133 *Overlap of variants with >5% minor allele frequency (MAF) in the GTEx dataset that overlap various eQTL and TF annotations.*
134 *Percent is based on all 5% MAF variants. Filtering eQTL variants for TF binding sites based on TF ChIP-seq peak overlaps and TF*
135 *motif matches still results in a large number of potentially causal eQTL variants.*

136 Interaction of eQTL effects and TF expression levels within tissues

137 We first investigated how inter-individual variation in TF levels within a tissue impacts eQTL effect
138 size, with the hypothesis that such effects could represent TF regulators of specific eQTLs. We chose 20
139 diverse tissues that best represented all 49 GTEx eQTL tissues based on gene expression clustering [SFig.
140 3]. For each of those tissues and each of our 169 TFs, we applied a linear regression with an interaction
141 term to discover TF level - genotype interactions on gene expression for our filtered variants across 32,151
142 genes, selecting the top eQTL variant per gene for each analysis [31] [Fig.1E,F]. We discovered 13 to 39,693
143 TF-eQTLs (eQTLs with TF interaction) per tissue at a 20% TF-level Benjamini-Hochberg (BH) FDR, with
144 133,111 relationships supported by at least one tissue [SFig. 4]. These TF-eQTL pairs represent potential
145 TF regulators of eQTL effects.

146 We observed that five tissues (Whole Blood, Fibroblast, Colon, Stomach, and Testis) were outliers
147 in the number of TF-eQTLs, which could not be explained by tissue sample size alone [SFig. 4]. Analysis of
148 *in silico* cell type estimates revealed that four of these tissues (Whole Blood, Fibroblast, Colon, and

149 Stomach) had particularly high inter-individual variability in cell type composition [SFig. 5]. Assuming that
150 this high cell type composition variability was likely contributing to the large number of TF-eQTLs, we
151 removed these tissues from our analysis so that our TF-eQTL results were not dominated by non-causal
152 correlations of TFs with cell type composition. We also removed the Testis tissue due to its outlier status
153 in previously reported gene expression and *trans*-regulation analyses [1,4], so that TF-eQTLs in this one
154 tissue would not dominate the results.

155 Our final within-tissue dataset consisted of 26,038 TF-eQTL relationships supported by at least
156 one tissue, of which 2,315 were supported by multiple tissues [Fig. 2A; SFig. 6]. Some TFs with many
157 interacting eQTLs in a tissue made clear biological sense. For instance, the TFs with the most interactions
158 in Brain Cortex and Nucleus Accumbens tissues were BCL11A and MEF2D, respectively, both of which are
159 involved in neuronal functions [32,33], and the TF with the most interactions in Adipose tissue was CEBPA,
160 which is a key driver of adipogenesis [34] [Fig.2A]. We see that 90/120 tissue pairs were enriched for one
161 another's TF-eQTLs (OR = 14.1 to 2251, Fisher's exact test, all $p < 0.05$) [Fig. 2C]. All those pairs with a
162 negative direction of enrichment included a brain tissue and/or the lymphoblastoid cell line and did not
163 have any overlapping TF-eQTL interactions, likely due to the small sample sizes and these tissue types
164 being highly distinct from others (all ORs = 0, Fisher's exact test ps = 1) [5]. In general, within-tissue TF-
165 eQTL relationships follow a similar clustering pattern to tissue gene expression [SFig. 3]. These results
166 highlight unique and shared potential TF regulators of eQTL effects within different tissue contexts.

167 Correlation of eQTL effect sizes and TF levels across tissues

168 To obtain further insights into TFs driving eQTL effect size variation between tissues, we next
169 investigated how TF levels across the 49 GTEx tissues correlated with eQTL effect sizes. We calculated log2
170 allelic fold change effect sizes (aFCs) in every GTEx tissue for each filtered variant-gene pair; by ignoring
171 eQTL significance cutoffs, we captured tissues lacking eQTL effects and avoided power differences in eQTL

172 detection caused by varying tissue sample sizes. We correlated aFCs for each eQTL with expression levels
173 for each of 169 TFs [Fig. 1D] and selected the top eQTL variant per gene for each TF. We found 420,248
174 TF-eQTL correlations at a 5% TF-level BH FDR [Fig. 2B]. These TF-eQTL pairs represent potential TF
175 regulators of eQTL effects that may explain the variability of these eQTLs across tissues. Many of the TFs
176 with the most correlations in the cross-tissue analysis were involved in immune (ELF1, IRF2, RELB, STAT3,
177 RELA) or hormone response (THRA) [35–39] [Fig.2B]. Though we discovered many more potential TF-eQTL
178 relationships across tissues than within tissues, the two sets of TF-eQTL interactions are enriched for one
179 another (OR = 2.43, Fisher's exact test $p < 10^{-300}$), and cross-tissue correlations showed a positive direction
180 of enrichment for all individual tissues except brain cerebellum [Fig. 2C].

181 Gene expression levels do not always directly correspond to protein levels [40,41], so we
182 performed a similar correlation analysis using TF protein levels across tissues, as assessed by high-
183 throughput mass spectrometry [42]. Protein quantification was available for 72/169 TFs in 20 or more
184 tissues, with one to 11 samples per tissue [STable 1]. We discovered 12,289 TF protein-eQTL correlations
185 at a 20% TF-level BH FDR [Fig. 2B]. These protein-based TF-eQTL correlations were not enriched for
186 expression-based cross-tissue or within-tissue TF-eQTL correlations (OR = 0.95, 0.47; Fisher's exact test p
187 = 0.097, 7.9×10^{-7}, respectively) [Fig. 2C, SFig. 7]. As discussed in Jiang et al., gene and protein levels may
188 differ due to biological phenomena of RNA dynamics and translational regulation as well as technical
189 variation in mass spectrometry technology that plagues especially lowly expressed proteins [42]. Given
190 that TF protein levels are lower than other genes (Wilcoxon rank sum test $p < 10^{-300}$) [SFig. 8] and the
191 number of assayed tissues and samples is small, these protein measurements may be less suitable
192 measurements of TF levels for the purposes of this analysis.

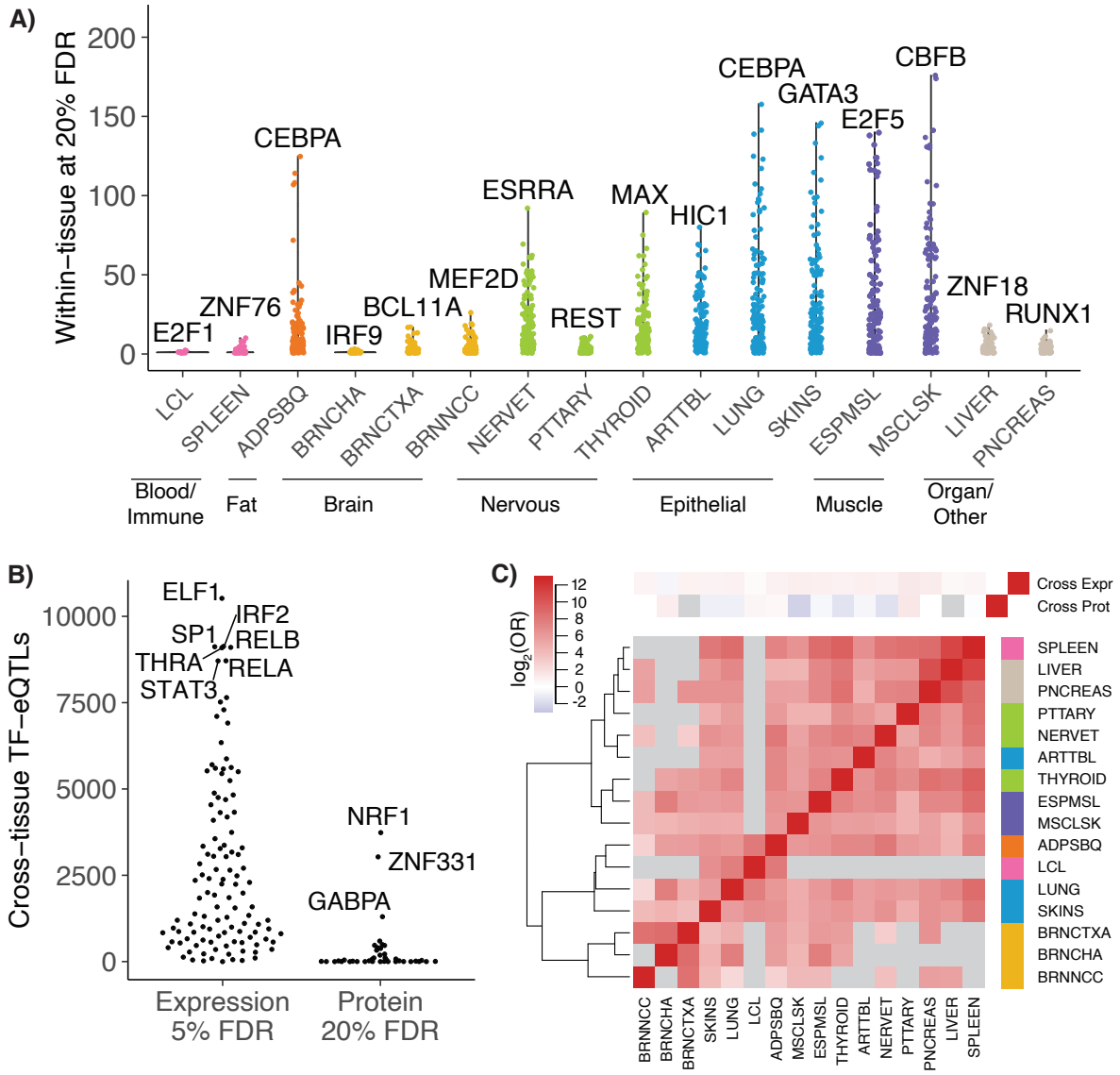

Figure 2. Discovered TF-eQTL interactions. A) *Number of within-tissue TF-eQTL interactions at 20% FDR is plotted per TF for each tissue analyzed. The TF with the most interactions per tissue is highlighted.* ***B)*** *Number of discovered cross-tissue TF-eQTL interactions per TF for expression-based interactions (at 5% FDR) and for protein-based interactions (at 20% FDR). TFs with the most correlations per analysis are highlighted.* ***C)*** *Sharing of TF-eQTL interactions between tissues and within/cross-tissues. Red indicates positive enrichment and blue, negative enrichment. Grey squares indicate no shared TF-eQTL gene pairs between the two datasets.*

Annotation and TF-binding of TF-eQTL interactions

Next, we set out to evaluate our discovered sets of putative TF regulators of eQTLs, based on orthogonal data of functional annotations and TF binding. We examined four TF-eQTL datasets: cross-tissue expression-based, cross-tissue protein-based, within-tissue expression-based, and at least two lines of expression-based evidence (at least two tissues, or cross-tissue + at least one tissue). First, we examined genomic annotations of the top TF-eQTL variant for each gene and found that all three expression-based datasets were enriched to overlap promoters, 5' UTR, and 3' UTRs compared to all tested eQTL variants [SFig. 9]. This is consistent with overall eQTL enrichments [1,4], suggesting that TF-eQTL variants are further enriched for true causal regulatory variants.

We tested whether our four sets of putative TF-eQTL interactions overlapped TF binding sites (TFBS) based on two datasets: ENCODE TF ChIP-seq peaks and HOCOMOCO predicted TF binding motifs. The top TF-eQTL variants showed enrichment for TF ChIP-seq overlap in most datasets and mixed results on TF motif matching enrichment [SFig. 10]. Given the complicated structure of our data, with multiple variants tested per gene and LD between variants [SFig. 2, 11], we set up a more sophisticated test of TFBS overlap enrichment of TF-eQTL interactions to account for this unusual data structure. We compared the observed overlap per gene to a null expectation and calculated significance using a permutation scheme of TFBS overlap annotations (see *Methods*). Our enrichment statistic can be interpreted as the average number of extra variants with overlap per TF-eQTL gene. Both cross-tissue and within-tissue expression-based datasets were significantly enriched for ChIP-seq overlap (cross-tissue enrichment statistic = 0.024, $p < 2x10^{-4}$; within-tissue enrichment statistic = 0.053, $p = 8x10^{-4}$), and cross-tissue expression-based TF-eQTLs showed a small trend of motif matching enrichment (enrichment statistic = 0.004, p = 0.06) [Fig. 3A; SFig. 11]. TF-eQTLs with at least two lines of expression-based evidence did not reach nominal significance for ChIP-seq overlap or motif matching, but they showed a similar magnitude of enrichment to the individual datasets [Fig. 3A; SFig. 11]. The cross-tissue protein-based TF-eQTL interactions had low

224 enrichment for ChIP-seq overlap and motif matching [Fig. 3A; SFig. 10, 11]; thus, taken together with their
225 low concordance with expression-based interactions [Fig. 2C], we decided not to pursue these
226 interactions any farther.

227 Though our discovered expression-based TF-eQTL relationships were generated using only
228 genetic and gene expression data, those eQTLs were more likely to overlap a TFBS of their interacting TF
229 than expected [Fig. 3A]. We included all TF-eQTL interactions with at least two lines of expression-based
230 evidence to represent a high-confidence set of putative TF regulators of genetic variant effects. These TF-
231 eQTL genes were also enriched to fall into the regulon of the interacting TF (any regulon set OR = 1.54,
232 Fisher's exact test $p = 1x10^{-17}$) [43], with the strongest enrichment seen for regulons defined by co-
233 expression analysis (OR = 2.08, Fisher's exact test $p = 1x10^{-22}$) [Fig. 3B]. These 6,262 dual-evidence TF-eQTL
234 interactions, observed across 154 TFs and 1,598 genes, represent potential TF regulators of genetic variant
235 effects [STable 2] that we then analyzed further.

236 Allele-specific TF binding of dual-evidence TF-eQTL interactions

237 We next examined TF ChIP-seq allele-specific binding data to determine if our dual-evidence TF
238 regulators of genetic variant effects manifested altered TF binding *in vivo*. To accomplish this, we used the
239 ADASTRA dataset, which contains allele-specific TF binding (ASB) results from over seven thousand TF
240 ChIP-seq experiments, normalized for cell-type-specific background allelic dosage [44]. Like our TFBS
241 overlap enrichment analysis, we compared the observed allele-specific TF binding of TF-eQTL interactions
242 to a null expectation, followed by permutation of ASB annotations to estimate the enrichment
243 significance.

244 We observed that TF-eQTL variants were significantly more likely to have ASB in general, with any
245 TF (enrichment statistic = 0.09, p=0.002) [Fig. 3C]. Testing for the enrichment of ASB for the matching TF-
246 eQTL TF was limited by the sparsity of the ASB data: only 9 out of 124 analyzed TFs were expected to have

247 more than one interacting TF-eQTL with an ASB event [SFig. 13]. However, 8/9 of these TFs showed more
248 ASB than expected, though none to a significant degree [Fig. 3C], and the overall enrichment was modest
249 but again non-significant (enrichment statistic = 0.011, p=0.10). These results demonstrate that our dual-
250 evidence TF-eQTL interactions are enriched for variants that alter TF binding, though these data are too
251 sparse to validate this specifically for the implicated TF.

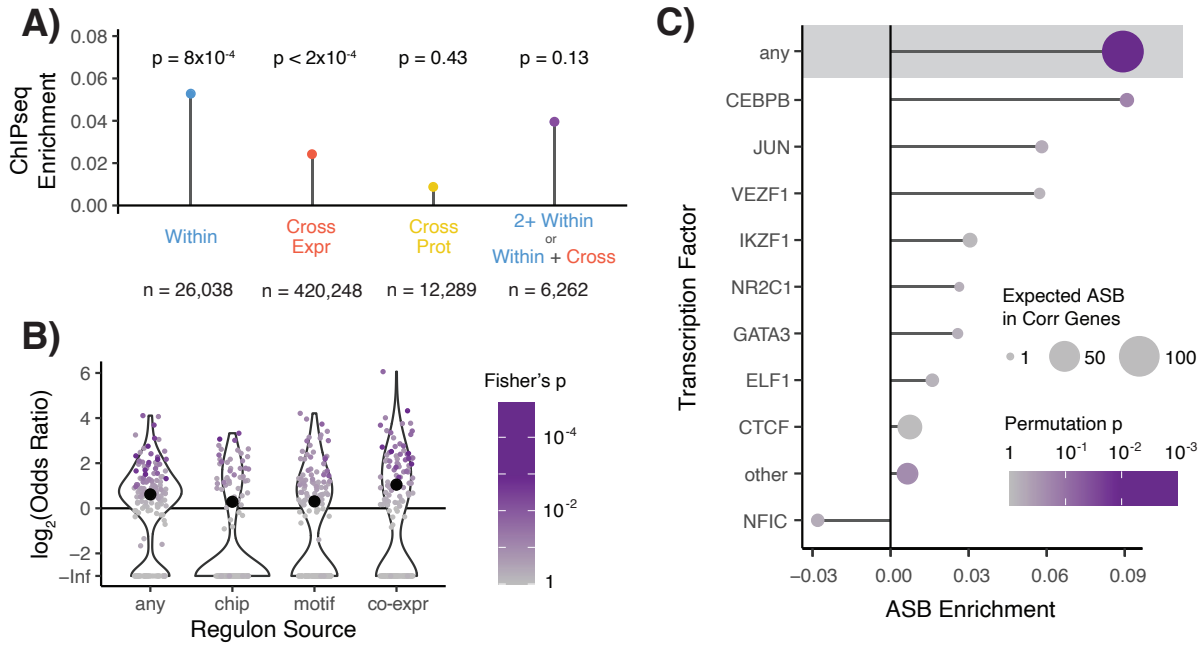

252

253 ***Figure 3. TF binding of TF-eQTL interactions. A)*** *Overlap enrichment of TFBS, based on TF ChIP-seq peaks, of TF-eQTL interactions*
254 *by dataset. Permutation-based p-values are plotted above each measurement. Datasets include within-tissue (blue) interactions,*
255 *cross-tissue expression-based (red), cross-tissue protein-based (yellow), and TF-eQTL interactions with at least two lines of*
256 *evidence from cross-tissue expression-based and within-tissue interactions (purple).* ***B)*** *The enrichment of target genes with two*
257 *lines of evidence for TF-eQTL interactions falling into that TF's regulon. Large black dots depict overall enrichment across TFs.* ***C)***
258 *Enrichment for allele-specific TF binding (ASB) for TF-eQTL interactions with two lines of evidence. Shaded area contains statistics*
259 *for unmatched TF ASB analysis. Below that, statistics for matched TF ASB analysis is shown, with TFs with more than one expected*
260 *ASB event plotted individually, and all other TFs combined (other).*

261 ## IRF1 knockdown validates IRF1-eQTL interactions

262 Our dual-evidence TF regulators included 58 eQTL effects putatively regulated by IRF1, which we
263 assessed further with an IRF1 knockdown experiment. We used data from a CRISPR-interference-
264 mediated knockdown of IRF1 in HEK293-TLR4 cells [45] and measured genes' allele-specific expression
265 (ASE) at knocked-down and control IRF1 levels [Fig. 4A,B]. A change in ASE between IRF1 conditions would
266 suggest that IRF1 is regulating the effect of the heterozygous eQTL on gene expression.

267 We compared allele-specific gene expression in IRF1-knockdown and control cells, combining
268 reads across all samples per condition to increase our power to discover differences in allelic expression.
269 After filtering for sufficient coverage of a heterozygous coding SNP (>60 reads, >5% REF reads, >5% ALT
270 reads, and <5% non-REF/ALT reads), we were left with 1,221 genes for which we performed Fisher's exact
271 test for imbalanced allelic expression across conditions. A low Fisher's test p-value indicates that the two
272 alleles are expressed at different ratios in the knockdown and control conditions, suggesting that IRF1
273 controls the expression of the gene in an allele-specific manner in this cell line.

274 We discovered 87 nominally significant genes with differing ASE between IRF1 conditions (Fisher's
275 exact test $p < 0.05$). These genes were significantly enriched to overlap our previously discovered IRF1-
276 eQTL genes (dual evidence TF-eQTLs OR = 8.03, Fisher's exact test $p = 0.015$) [Fig. 4C]. Of the dual-evidence
277 TF-eQTL genes with measurable ASE, all seven were heterozygous for an implicated top IRF1-eQTL variant,
278 thus we could expect all to show differing ASE between IRF1 conditions. Indeed, three genes, *ERI1*,
279 *MYOM2*, and lncRNA *RP5-1092A3.4* were nominally significant, and all seven genes had p values in the
280 lower quartile of tested genes, with a maximum p value of 0.31 [Fig.4E; SFig. 14, 15]. Examining ASE in this
281 IRF1 knockdown experiment validated 3/7 of our testable IRF1-eQTL interactions and demonstrates the
282 high promise of this method to generate useful TF regulation information that can be applied to
283 understand allele-specific regulation in new contexts.

284

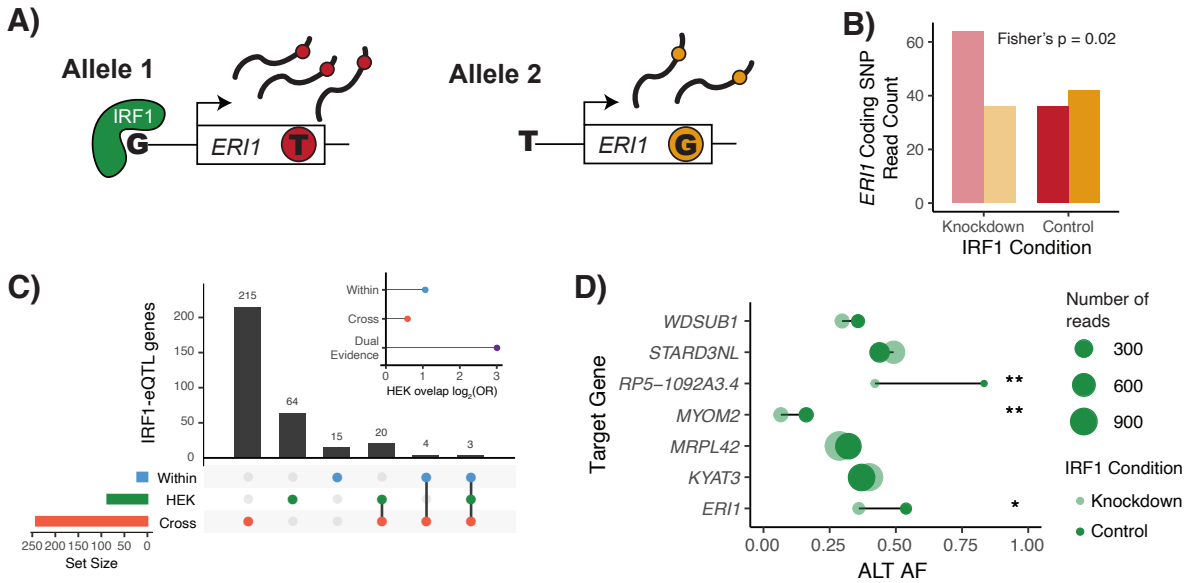

***Figure 4. IRF1-eQTL interactions in HEK293-TLR4 IRF knockdown**. **A)** Depiction of allele-specific expression, with IRF1 preferentially binding to the G-allele in the regulatory region of the ERI1 target gene. This leads to higher expression of allele 1, which we can measure based on the presence of a heterozygous coding SNP in the ERI1 transcript. Reads from allele 1 will have a T genotype (red) at the coding SNP and reads from allele 2 will have a G (orange). **B)** Read counts for ERI1 coding SNP alleles in both knockdown and control conditions. In this example, it appears that we observe allelic effects at lower (knockdown) IRF1 levels, while higher (control) levels of IRF1 may saturate binding to both alleles. Conditions are compared using Fisher's exact test of allelic counts. **C)** Sharing of IRF1-interacting eQTL genes in within-tissue (blue), cross-tissue expression-based (red), and HEK293 IRF1 knockdown (green) datasets. Only genes with an adequately expressed heterozygous coding SNP in HEK293 samples are included. Inset shows enrichment for overlap between HEK293T IRF1-eQTL genes and listed datasets. **D)** HEK293 coding SNP alternative allele frequency in dual-evidence IRF1-eQTL genes that were heterozygous for a top TF-eQTL variant and had adequate coverage of a heterozygous coding SNP. * indicates a Fisher's p value < 0.05, ** < 0.01 of allelic counts vs. condition.*

TF regulation of gene-by-environment effects and genetic effects on phenotype

We hypothesized that our TF-eQTLs could shed light on mechanisms of gene-by-environment (GxE) interactions that represent environmental conditions that affect genetic control of a phenotype, and altered TF level could be the mechanism by which the environmental condition regulates the genetic effects. In a recent large-scale study, Findley et al. tested the effects of 14 environmental treatments on

302 allele-specific gene expression in three cell lines, discovering 979 genes with GxE effects, 850 of which
303 were also found to have a GxE interaction by a previous study [12]. We overlapped our dual evidence TF-
304 eQTL genes with these replicated GxE interacting genes and found 92 overlaps (OR = 2.67, Fisher's exact
305 test $p = 1.4x10^{-14}$) [Fig. 5A], which offer potential direct mechanistic interpretations of the environmental
306 effects on genetic control of gene expression [STable 3]. For instance, we found multiple GxE interactions
307 for copper treatment that overlapped TF-eQTL genes for MITF or RELA; both TFs have been found to
308 respond to copper exposure [46,47], thus they could be the mechanism by which copper regulates genetic
309 effects at these loci. Thus, combining TF-eQTL mechanisms with GxE interactions therefore has the
310 potential to elucidate direct mechanisms of environmental effects.

311 We next assessed if we could use our TF-eQTLs to discover TF regulators of GWAS loci.
312 Colocalization methods can combine statistical signals from eQTLs and GWAS loci to determine if the gene
313 and phenotype regulation share a causal variant, implying that genetic regulation of the gene may be the
314 causal mechanism of the genetic effect on phenotype. We obtained GWAS-eQTL colocalization data of
315 GTEx eQTLs and 76 GWAS traits [48,49] and combined these with our dual-evidence TF-eQTLs. We saw
316 that our TF-eQTL genes were more likely to colocalize with GWAS loci than all tested eQTL genes, with
317 27% of our TF-eQTL genes showing colocalization between a GWAS signal and an eQTL in any tissue and
318 9.5% showing colocalization between a GWAS signal and an eQTL in the same tissue where the TF-eQTL
319 was discovered (OR = 2.00, 1.65, Fisher's exact test $p = 2.1x10^{-29}$, $1.1x10^{-10}$, respectively) [Fig. 5B]. We
320 found 205 colocalizations between a GWAS signal and an eQTL signal in a tissue with a dual evidence TF-
321 eQTL that had high LD between the lead colocalization and TF-eQTL variants ($r^2 > 0.4$), which represent
322 potential TF regulators of genetic effects on phenotype [STable 3].

323 One example of this relationship is an *APBB1IP* eQTL that interacts with transcription factor IKZF1.
324 This eQTL is present in 31 GTEx tissues and colocalized with GWAS signals for four red and white blood
325 cell traits (ENLOC regional conditional probability > 0.5), suggesting that genetic control of these traits

326 could be mediated by *APBB1IP* expression [48–50] [Fig. 5C; SFig. 16; STable 4]. We observed three tissues
327 (pituitary gland, thyroid, and tibial artery) with TF-eQTL interactions for the *APBB1IP* gene with IKZF1
328 [51,52] [Fig. 5D,E; SFig. 17]. Supporting IKZF1 regulation of this eQTL, the top TF-eQTL and GWAS variants
329 were highly linked ($r^2 > 0.85$) to *rs1335540*, a SNP found 15 bases upstream of an *APBB1IP* transcript start
330 site that overlaps an IKZF1 ChIP-seq peak and matches a IKZF1 motif [53–55] [Fig. 5F, SFig. 17, 18]. *APBB1IP*
331 eQTLs in all three tissues with an IKZF1-eQTL interaction showed colocalization with blood cell traits.
332 *APBB1IP* mediates blood cell adhesion and immune response [56,57]. It is also involved in integrin-
333 mediated changes in the actin cytoskeleton of mammalian cells [58,59] and its orthologue MIG-10 has
334 been shown to regulate axon outgrowth in *C. elegans* neurons [60]. IKZF1 is a chromatin-remodeling TF
335 involved in lymphocyte development as well as the neuroendocrine system [51,52]. These findings offer
336 two explanations for the genetic control of blood cell traits by *APBB1IP* expression: 1) via altered gene
337 expression in the blood cells themselves, or 2) via neuroendocrine control of blood cell counts originating
338 with altered gene expression in neurons. Offering further support to the neuroendocrine hypothesis,
339 thyroid dysfunction has been shown to alter red and white blood cell counts [61,62], and the IKZF1-eQTL
340 interactions were observed in neuroendocrine tissues. Regardless, given the shared genetic signal in
341 multiple tissues, we can hypothesize that IKZF1 regulates both *APBB1IP* expression and the implicated
342 blood traits, suggesting a TF regulator of a complex trait's genetic association.
343

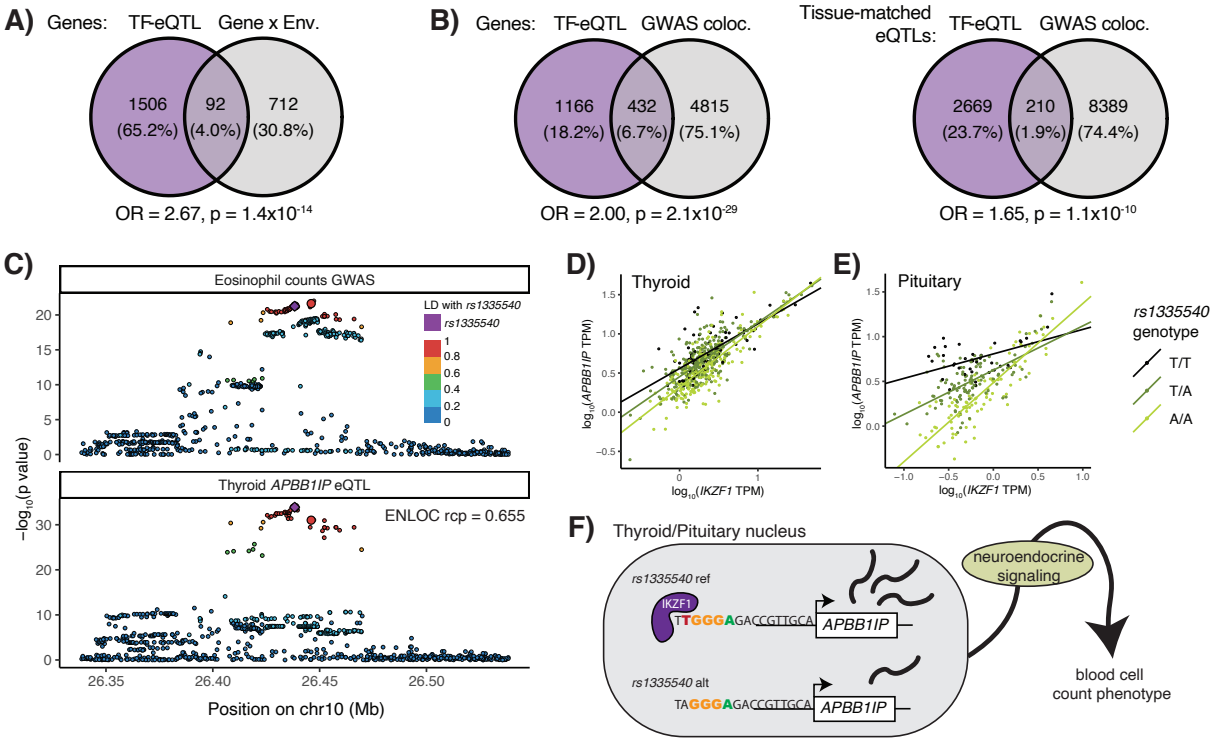

***Figure 5. TF-eQTL implications for gene-by-environment and GWAS effects**. **A)** Overlap of TF-eQTL genes with GxE genes from Findley et al. 2021. **B)** Overlap of TF-eQTL genes with GWAS colocalizing eQTL genes from GTEx. The first diagram shows overlap for a gene with a TF-eQTL in any tissue and colocalizing eQTL in any tissue. The second shows overlap of tissue eQTLs with TF-eQTL and/or colocalizing GWAS locus in the given tissue. **C)** Representative eQTL and GWAS p-values are plotted for variants in the region of an* APBB1IP *eQTL and blood trait GWAS locus. Lead variants from IKZF1-eQTL interactions in thyroid, pituitary, and tibial artery are larger and outlined in black. (The lead variant from pituitary/artery cannot be seen as it falls behind* rs1335540.*) **D)** & **E)** Individual samples in thyroid and pituitary tissues are plotted by* IKZF1 *and* APBB1IP *expression, and linear regression lines are plotted by genotype. The difference in APBB1IP expression between the genotypes gets smaller as IKZF1 expression increases across the samples. **F)** Schematic of IKZF1 regulation of APBB1IP and blood cell counts. An IKZF1 binding site predicted by the HOCOMOCO IKZF1 motif lies nine bases upstream of APBB1IP's transcription start site, which is disrupted by the alternative allele of rs1335540. Under our neuroendocrine signaling hypothesis, APBB1IP expression in neuroendocrine tissues goes on to alter system-wide neuroendocrine signaling, which would cause changes in blood cell counts. As IKZF1 appears to regulate the APBB1IP eQTLs in these tissues, it would follow that IKZF1 TF therefore may regulate the effect of this locus on blood cell counts.*

358 # Discussion

359 In this paper, we used the natural variation of TFs across tissues and individuals to discover 6,262
360 TF-eQTL interactions across 1,598 genes, which represent putative TF-based mechanisms of genetic
361 effects on gene expression. These TF-eQTLs were supported by at least two lines of evidence, including
362 cross-tissue and/or within-tissue variation. They were enriched to overlap ChIP-seq peaks and fall into the
363 regulon of the implicated TF, corroborating with orthogonal evidence that these eQTLs are regulated by
364 the implicated TFs. Furthermore, analysis of an IRF1-knockdown experiment validated three out of seven
365 testable IRF1-eQTLs. We see that TF-eQTL genes are more likely to colocalize with GWAS loci and overlap
366 genes with gene-by-environment effects, and our example of IKZF1 regulation of an *APBB1IP* eQTL that
367 colocalizes with GWAS signals for blood cell traits illustrates how our TF model can be used to discover
368 likely TF regulators of GWAS effects.

369 Given the high number of possible causal genetic variants and putative regulatory mechanisms
370 based on statistical fine-mapping and functional annotation overlap, it is clear that additional methods
371 are needed to pinpoint causal variants and mechanisms of quantitative trait loci. Our method offers a new
372 approach to discovering TF regulation of a genetic variant's effects, which can help us determine the
373 eQTL's potential mechanism of action and explain its context variability. One major advantage to our
374 method is its accessibility. While functional annotations were used to choose variants to test and to
375 validate our results, the main discoveries of the model were powered by sample genotypes and gene
376 expression levels – the same data available in most eQTL analyses. We leverage variation cross-tissues
377 and within-tissues, which both have value for discovering TF regulators of eQTL effects, but especially the
378 within-tissue TF interaction analysis is applicable to any eQTL data set even when a large number of
379 different conditions may not be available.

380 Understanding TF regulation of an eQTL effect can allow us to focus functional fine-mapping
381 efforts only on the implicated TF, hopefully narrowing the focus to one or a handful of variants that disrupt

382 binding sites predicted by that TF's motif or show allele-specific binding in its ChIP-seq data. Unlocking
383 these mechanisms allows us to eventually improve our understanding of the regulatory code of the
384 genome and how human genetic variation perturbs that system. One clear application of our approach is
385 for discovering and interpreting gene-by-environment (GxE) effects on gene expression and phenotype.
386 While GxE interactions on human phenotype have been difficult to assess, GxE interactions in relation to
387 gene expression have been studied under various contexts [8,12–15,63–65]. Overlapping these effects
388 with TF-eQTLs as in our analysis, or even performing TF-eQTL analysis in the environmental exposure
389 datasets themselves, provides mechanistic hypotheses of how environmental effects impact genetic
390 control of gene expression and phenotype.

391 We were surprised by the lack of validation of TF-eQTLs discovered with cross-tissue protein
392 levels, since protein measurements should reflect TF activity levels more accurately than expression
393 measurements. However, the protein data had less power, from a smaller number of individuals and
394 tissues than the expression data, and mass spectrometry may have more technical noise than expression
395 quantifications from RNA-seq. Another promising option for TF measurement in the model is TF activity
396 as predicted by target gene expression [66], which should account for translation rates, post-translational
397 modifications, and subcellular localization effects on TF activity that expression measurements cannot
398 capture. Initial analyses with this datatype did not yield strong results, but as activity estimates improve,
399 the option should be revisited.

400 Though we saw enrichment for TF ChIP-seq peaks and allele-specific binding, our TF binding
401 enrichments were quite modest. For instance, the TF ChIP-seq overlap enrichment statistic of 0.05 for
402 dual-evidence TF-eQTLs means that we observed 0.05 more variants with ChIP-seq overlap per TF-eQTL
403 gene than expected – or one additional overlap per twenty genes. Part of this may arise from the lack of
404 ChIP-seq data from relevant tissue and cell type contexts that match the GTEx eQTL data. Nonetheless, it
405 is likely that our dual-evidence TF-eQTLs likely contain false positives. One of the factors that may

406 contribute to this is the correlated expression between TFs, which is difficult to fully account for. Another
407 important factor is TF-eQTL correlations that may be caused by cell type composition [6], such that an
408 eQTL only found in a given cell type might be correlated with TFs that are highly expressed in that cell type
409 even when the TF does not specifically regulate the eQTL. While some of our discovered TF-eQTLs may be
410 false positives due to cell type variability, the ChIP-seq enrichments and IRF1 validation indicate that the
411 applied filters successfully remove many of the major cell type composition effects. Altogether, we
412 consider our 6,262 TF-eQTLs to represent regulatory variants with an indication of being regulated by the
413 implicated TFs, but full validation will require additional work.

414 In summary, in addition to this catalog of potential TF regulators of eQTLs, we hope that our
415 methods of comparing TF level with genetic variant effect can be applied in additional eQTL datasets, as
416 well as for splicing QTLs and other molecular phenotypes. Our approach has the potential to implicate
417 mechanisms for eQTL effects that vary across contexts without requiring additional datatypes or
418 experiments, though its integration with other lines of evidence can further strengthen the insights, as
419 shown in this study. Additionally, our method can improve functional fine-mapping efforts by highlighting
420 TFs that may be regulating a locus, which can be further investigated with functional genomic data for
421 that TF such as motif prediction or allele-specific binding data. We believe this TF-based framework of
422 genetic variant effect variability can advance our understanding of QTL and GWAS mechanisms and their
423 context variability, with great promise for understanding environmental interactions that impact genetic
424 disease risk.

Methods

GTEx data

For the bulk of our analysis, we used the GTEx v8 dataset, including whole genome sequencing for 838 individuals and mRNA sequencing from 15,201 samples across 49 tissues [Table 2, STable 1]. RNA-seq data were aligned using STAR v2.5.3a, and gene counts were based on GENCODE Release 26 and analyzed using RNA-SeQC [5]. *cis*-eQTL calculations in each tissue and Caviar fine-mapping 95% confidence sets for those eQTLs were also previously generated [Table 2] [5]. High-throughput mass spectrometry protein measurements were separately available for 201 GTEx samples across 32 tissues [42] [Table 2, STable 1]. GTEx tissues were categorized into Blood/Immune, Adipose, Brain, Nervous System (non-brain), Epithelial, Muscle, or Organ/Other via a cursory literature search on biological composition and function.

Table 2. Data Sources.

Data Type	Publication DOI / Citation	Website
GTEx v8 genetic, gene expression, eQTL, and fine-mapping data	10.1126/science.aaz1776 / [5]	https://gtexportal.org/home/
GTEx protein data	10.1016/j.cell.2020.08.036 / [42]	
GTEx GWAS colocalization	10.1186/s13059-020-02252-4 / [49]	
ENCODE TF ChIPseq peaks	Multiple experiments	https://www.encodeproject.org/search/?type=Experiment
HOCOMOCO TF motifs	10.1093/nar/gkx1106 / [54]	https://hocomoco11.autosome.ru/
ADASTRA allele-specific binding data	10.1038/s41467-021-23007-0 / [22]	https://adastra.autosome.ru/susan
HEK293-TLR4 IRF1 knockdown experiment	10.1101/2020.02.21.959734 / [45]	
HEK293-TLR4 genome sequence	10.1038/ncomms5767 / [67]	http://hek293genome.org/v2
Gene-by-environment interactions	10.7554/eLife.67077 / [12]	

438 ## Filtering variants

439 We limit our analysis to variants where we have prior evidence to suggest that this could be a
440 variant affecting gene expression that is regulated by a TF. We filtered for variants that matched four
441 criteria: 1) >=5% minor allele frequency in GTEx v8 samples; 2) present in a Caviar fine-mapped 95%
442 credible set for an eQTL in any GTEx tissue; 3) overlap an ENCODE TF ChIP-seq peak for at least one of 169
443 TFs; 4) match a HOCOMOCO consensus sequence motif for at least one of 169 TFs. We used ENCODE
444 narrowPeak regions in all available experiments that passed filtering criteria (as of January 2020) and
445 HOCOMOCO v11 IUPAC consensus motifs [Table 2]. For the ENCODE TF ChIP-seq overlap, we used ChIP-
446 seq optimal irreproducible discovery rate (IDR) threshold peak files for experiments with a biological
447 replicate, no red or orange audit categories, and no experimental conditions. We used a union of regions
448 if multiple IDR files were available per TF. For HOCOMOCO TF motif matching, we converted the IUPAC
449 consensus sequence motif to a regular-expression string for both the forward and reverse-compliment
450 motif, trimming any less confident bases (lowercase letters) from the ends of the sequence. We extracted
451 the genomic sequence surrounding each variant (motif length minus one on either side of the variant)
452 using samtools, and we used grep to check if the forward or reverse-compliment motif was present in the
453 reference and/or the alternative alleles. The above filtering left us with 473,057 variants. Using the Caviar
454 fine-mapping data, we associated each filtered variant with one or more eGenes, which resulted in
455 1,032,124 eVariant-eGene pairs across 32,151 genes.

456 ## Within-tissue interactions

457 For our within-tissue TF-eQTL interaction discovery, we selected twenty tissues that best
458 represented all 49 GTEx eQTL tissues based on gene expression clustering. We clustered tissues based on
459 median TPM across all genes using Euclidean distances and Ward.D clustering, cut the resulting tree to
460 generate twenty clusters, and selected the tissue with the largest sample size from each cluster. If a tissue

461 was removed for cell type composition variability (below), the next largest tissue was selected from the
462 cluster, if one was available.

463 For each selected tissue, we applied an eQTL interaction model to discover TF-eQTL interactions
464 on gene expression. We ran tensorQTL software per TF and per tissue for 32,151 genes and all filtered
465 variants within a 10 mega-base window of the transcription start site, inputting individuals' genotypes,
466 normalized eGene expression, and normalized TF expression for each eQTL-TF pair, as well as genotype
467 principal components and tissue covariates described in The GTEx Consortium, 2020 [5]. TensorQTL
468 software applied a gene-level p-value correction based on the effective number of independent variants
469 tested per gene, estimated with eigenMT (emt), and selected the variant with the lowest p-value per gene
470 [31,68]. We then applied a Benjamini-Hochberg (BH) correction to the emt-corrected p-values across each
471 tissue and TF. For all TF-eQTL interactions with BH FDR <= 20%, we selected those where the top TF-eQTL
472 variant had a significant eQTL signal in the respective tissue and where the gene was not the implicated
473 TF.

474 We removed four tissues with high cell type composition variability so that our results were not
475 dominated by non-causal TF-eQTL relationships due to cell type composition (Whole Blood, Fibroblast,
476 Colon, Stomach), and we removed one tissue due to its high number of results and unique gene expression
477 patterns (Testis). Cell type composition was estimated in Kim-Hellmuth et al., 2020 [6]: briefly, XCell was
478 used to calculate enrichment of cell-type-specific gene expression signals in GTEx samples [69]. Since
479 these estimates were not all experimentally validated, we ignored cell type estimates with high variability
480 across tissues (aDC, iDC) [SFig. 5]. Four cell type estimates had high variability in a GTEx tissue (variance >
481 0.04; Th2 cells in fibroblasts, epithelial cells in the colon, epithelial cells in the stomach, and basophils in
482 blood) and those tissues were removed from the analysis to avoid strong cell type interaction signals in
483 our results. Stomach clustered with other tissues [SFig. 4], so we added the next largest tissue in that
484 group, Pancreas, to our within-tissue TF-eQTL analysis.

485 ## Cross-tissue correlations

486 We correlated eQTL effect sizes and TF expression levels across up to 49 GTEx tissues. We used
487 the aFC software package to calculate eQTL effect sizes based on log2 allelic fold change (aFC) for all
488 eVariant-eGene pairs in each tissue [70], using genotype principal components and tissue covariates
489 described in The GTEx Consortium, 2020 [5]. We determined the median TF level per tissue based on
490 transcripts per million (TPM). Then we performed a cross-tissue Spearman correlation of eQTL aFC and TF
491 median TPM for each eQTL-TF pair in all tissues with median eGene expression greater than 0 TPM, i.e.,
492 in all tissues where the eQTL target gene was sufficiently expressed. We tested 1-249 eVariants per eGene,
493 and we selected the top variant per gene and calculated a corrected p-value using the effective number
494 of independent variants tested per gene. We defined the effective number of tests per gene as the
495 number of eigenvectors needed to capture 95% of the variance in the GTEx genotype matrix of all tested
496 variants, using the Gao method in the poolr package [71]. We then performed a Benjamini-Hochberg TF-
497 level correction of the meff-corrected p-values across the top variants of each gene, and we selected
498 variants with up to a 5% false discovery rate (FDR).

499 For our protein-based analysis, we used a similar approach, substituting TF protein levels for TF
500 expression levels. We examined median protein levels in 32 GTEx tissues using normalized high-
501 throughput mass spectrometry data [42]. We filtered for TFs with at least 20 unique protein values across
502 tissues, then performed a cross-tissue Spearman correlation of eQTL aFC and TF median protein level. We
503 tested 1,032,124 eQTLs and 72 TFs using the same p-value calculation procedure described above, then
504 selected variants with up to a 20% FDR.

505 ## Dataset comparison

506 We tested for TF-eQTL sharing across multiple datasets: cross-tissue expression-based, cross-
507 tissue protein-based, and each within-tissue expression-based dataset. We performed Fisher's tests based

508 on every TF-eGene pair's presence in the significant interactions from each dataset. For comparisons with
509 cross-tissue protein-based data, we only used TF-eGene pairs for 72 TFs tested in the protein data.

510 TF binding overlap enrichment

511 We tested whether our predicted TF-eQTL interactions overlap TF binding sites (TFBS) based on
512 two orthogonal datasets: ENCODE TF ChIP-seq peaks and HOCOMOCO predicted TF binding motifs [Table
513 2]. Given the complicated structure of our data, with multiple variants tested per gene and LD between
514 variants, we used an expectation/observation model to test TFBS overlap enrichment of TF-eQTL
515 interactions.

516 For each TF (*f*), we calculated the number of expected overlaps per gene (*g*) based on the number
517 of variants tested (*v*) and the probability that any variant overlapped that annotation (*p*), and compared
518 that to the observed number variants that overlap the annotation (*o*):

519 $$S_{f,g} = obs_{f,g} - exp_{f,g} = o_{f,g} - v_g * p_f \qquad \text{(Eq 1)}$$

520 We then averaged the per gene statistics across all genes with a significant TF-eQTL interaction (G_f):

521 $$S_f = \frac{\sum_{g \in G_f} S_{f,g}}{|G_f|} \qquad \text{(Eq 2)}$$

522 And we averaged across all 169 TFs to get our final enrichment statistic:

523 $$S_{overlap} = \frac{\sum_{f=1}^{169} S_f * |G_f|}{\sum_{f=1}^{169} |G_f|} \qquad \text{(Eq 3)}$$

524 The resulting statistic can be interpreted as the average extra number of overlaps per gene. For
525 instance, an overlap enrichment statistic of 0.01 would mean that we observed 0.01 more variants with
526 overlap per TF-eQTL gene than expected – or one additional overlap per 100 genes.

527 Permutations were carried out by shuffling overlap annotations across all tested variants and
528 recalculating the overlap statistic 10^4 times. Permutation p-values were calculated by counting the
529 number of times the permuted TF statistic is larger or smaller than the observed statistic, adding one,
530 dividing by the number of permutations, and multiplying by two for a two-sided test.

531 Allele-specific TF binding validation

532 We examined TF allele-specific binding (ASB) data to determine if our high-confidence set of
533 potential TF regulators led to altered TF binding *in vivo*. We based our analysis on the ADASTRA dataset
534 (Susan version), which contains a meta-analysis of allele-specific TF binding results from over 7,000 TF
535 ChIP-seq experiments [Table 2] [22]. Similar to our TFBS overlap enrichment analysis, we used an
536 expectation/observation model to test allele-specific binding of TF-eQTL interactions, then permuted
537 allele-specific binding annotations to calculate the enrichment significance.

538 For the un-matched TF ASB overlap analysis, we calculated the number of expected variants with
539 ASB per gene based on the number of tested variants that were assayed in the ASB dataset (v) and the
540 probability that any variant had ASB for any TF (p). We then compared the expected to the observed
541 number of variants with ASB (o) in each gene, and we averaged across all genes that had a significant TF-
542 eQTL interaction for any TF (G_{any}):

543 $$S_{any} = \frac{\sum_{g \in G_{any}} S_{,g}}{|G_{any}|} \quad \text{(Eq 4)}$$

544 For our matched TF analysis, we calculated the number of expected variants with ASB per gene
545 based on the number of tested variants that were assayed in the ASB dataset (v) and the probability that
546 any variant had ASB for the specified TF (p). We then compared the expected to the observed number of
547 variants with ASB (o) using the equation for S_g described previously (Eq 1), then averaged the per gene
548 statistics across all correlated genes using the equation for S_f (Eq 2).

549 The overall enrichment was calculated using S_g and S_f, with genes with a significant TF-eQTL

550 interaction per TF (G_f) and 124 total TFs, using the full equation:

551 $$S_{matched} = \frac{\sum_{f=1}^{124} \sum_{g \in G_f} o_{f,g} - v_g * p_f}{\sum_{f=1}^{124} |G_f|} \quad \text{(Eq 5)}$$

552 We then permuted ASB annotations across all tested variants and recalculated the ASB statistic

553 10^4 times. We calculated permutation p-values using the same two-sided test procedure described in our

554 TFBS overlap enrichment analysis.

555 IRF1 knockdown analysis

556 Our high confidence set of potential TF regulators included 58 eQTL effects predicted to be

557 regulated by IRF1. To test these, we used a CRISPR-i knockdown of IRF1 in TLR4-expressing HEK cells

558 (HEK293T) and measured allele-specific expression (ASE) at varying IRF1 levels [Table 2] [45]. If we observe

559 that ASE changes with IRF1 levels, this would suggest that IRF1 is truly regulating the effect of the eQTL

560 on gene expression. First, we filtered the aligned HEK293T RNAseq data for coding variants that had

561 adequate coverage to call ASE: at least 60 reads across all conditions, at least 5% reference allele and 5%

562 alternative allele, and less than 5% of other alleles. Then, we used Fisher's test to compare the allelic

563 balance across all promoter knockdown samples and all control samples. As our test was likely

564 underpowered, we looked at genes with a 0.05 nominal p-value cutoff. We then checked which IRF1-eQTL

565 top variants were heterozygous in the HEK293T cell line using VCF files from Complete Genomics [Table

566 2] [67]. All seven testable IRF1-eQTL were heterozygous for a top IRF1-eQTL variant in the HEK293T cell

567 line.

568 ## Comparison with GxE genes

569 Gene-by-environment interaction analysis results were attained from Supplemental Table 4 in
570 Findley et al., 2021 [Table 2] [12]. We matched these results by ENSG number with our dual-evidence TF-
571 eQTL genes and used Fisher's exact test to calculate overlap compared to all tested genes in our dataset.

572 ## GWAS colocalization

573 To discover TF regulators of GWAS loci, we examined colocalization of GTEx eQTLs and 76 GWAS
574 traits. We obtained ENLOC colocalization results (regional conditional probability > 0.5) from the GTEx
575 Consortium [Table 2] [48,49] and overlapped these eQTL genes with our high confidence TF-eQTL genes.
576 To test if our TF-eQTLs were enriched to colocalize with GWAS signals, we looked at all significant eQTL
577 genes in any tissue and performed a Fisher's exact test for whether or not the gene had an eQTL that
578 colocalized with a GWAS phenotype and whether or not we found a TF-eQTL interaction for that gene.
579 We also performed a tissue-specific analysis where we looked at all significant eQTL genes in the 16 tissues
580 where we performed within-tissue TF-eQTL discovery, and we performed a Fisher's exact test for whether
581 or not the tissue's eQTL signal colocalized with a GWAS phenotype and whether or not a high confidence
582 TF-eQTL was found for that gene in the tissue. Our list of 205 colocalizing GWAS-eQTLs with a TF-eQTL
583 were based on this tissue-specific comparison and were additionally filtered such that the r^2 of the top TF-
584 eQTL variant and the lead ENLOC colocalizing variant was great than 0.4.

585 # Supplementary Information

586 Supplementary tables 1-5 can be found in the supplementary Excel file.

587 Supplementary figures 1-17 and supplementary table legends can be found in the supplementary PDF.

Data and Code Availability

In addition to supplementary tables, additional relevant data tables as well as data analysis and plot-generation code are available at https://github.com/LappalainenLab/TF-eQTL.

Acknowledgments

We thank all members of the Lappalainen laboratory for their valuable discussions, and especially Stephane Castel, Margot Brandt, and Paul Hoffman for their data contributions. We thank the GTEx Consortium for their data, analyses, and expertise, including Andrew Brown and Farhad Homozdiari for their fine-mapping analyses, Lihua Jiang and Michael Snyder for access to GTEx protein data, and Hae Kyung Im, Alvaro Barbeira, and Rodrigo Bonazzola for the GWAS harmonization and colocalization efforts. We also thank Ivan Kulakovskiy and Vsevolod Makeev and their research teams for access to the ADASTRA allele-specific binding dataset.

This work was supported by NHGRI grant 5F31HG010580 (EDF); NIMH grant R01MH106842 (EDF, ALT, HJB, TL); Vagelos Precision Medicine Pilot Grant from Columbia University (EDF, HJB, TL); NHLBI grant R01HL142028 (SK, TL); Marie-Skłodowska Curie fellowship H2020 grant 706636 (SKH); Reinhard-Frank Stiftung and the Helmholtz Young Investigator grant VH-NG-1620 (SKH); NHLBI contract HHSN268201000029C (FA, KGA); NHGRI grant 5U41HG009494 (FA, KGA); NHGRI grant R01HG003008 (HJB); NIGMS grant R01GM140287 (PM); and NCATS grant UL1TR002550 (PM).

Competing Interests

TL advises Variant Bio, Goldfinch Bio, and GlaxoSmithKline and has equity in Variant Bio. FA is an inventor on a patent application related to TensorQTL.

References

1. The GTEx Consortium. The Genotype-Tissue Expression (GTEx) pilot analysis: Multitissue gene regulation in humans. Science. 2015;348: 648–660.

2. Gaffney DJ, Veyrieras J-B, Degner JF, Pique-Regi R, Pai AA, Crawford GE, et al. Dissecting the regulatory architecture of gene expression QTLs. Genome Biol. 2012;13: R7.

3. Kilpinen H, Waszak SM, Gschwind AR, Raghav SK, Witwicki RM, Orioli A, et al. Coordinated Effects of Sequence Variation on DNA Binding, Chromatin Structure, and Transcription. Science. 2013; 1–5.

4. GTEx Consortium, Aguet F, Brown AA, Castel SE, Davis JR, He Y, et al. Genetic effects on gene expression across human tissues. Nature Publishing Group. 2017;550: 204–213.

5. GTEx Consortium. The GTEx Consortium atlas of genetic regulatory effects across human tissues. Science. 2020;369: 1318–1330.

6. Kim-Hellmuth S, Aguet F, Oliva M, Muñoz-Aguirre M, Kasela S, Wucher V, et al. Cell type-specific genetic regulation of gene expression across human tissues. Science. 2020;369. doi:10.1126/science.aaz8528

7. Alasoo K, Rodrigues J, Mukhopadhyay S, Knights AJ, Mann AL, Kundu K, et al. Shared genetic effects on chromatin and gene expression indicate a role for enhancer priming in immune response. Nat Genet. 2018;50: 424–431.

8. Kim-Hellmuth S, Bechheim M, Pütz B, Mohammadi P, Nédélec Y, Giangreco N, et al. Genetic regulatory effects modified by immune activation contribute to autoimmune disease associations. Nat Commun. 2017; 1–10.

9. Ward MC, Banovich NE, Sarkar A, Stephens M, Gilad Y. Dynamic effects of genetic variation on gene expression revealed following hypoxic stress in cardiomyocytes. bioRxiv. 2020. pp. 1–42. Available: http://biorxiv.org/lookup/doi/10.1101/2020.03.28.012823

10. Dombroski BA, Nayak RR, Ewens KG, Ankener W, Cheung VG, Spielman RS. Gene expression and genetic variation in response to endoplasmic reticulum stress in human cells. Am J Hum Genet. 2010;86: 719–729.

11. Strober BJ, Elorbany R, Rhodes K, Krishnan N, Tayeb K, Battle A, et al. Dynamic genetic regulation of gene expression during cellular differentiation. Science. 2019;364: 1287–1290.

12. Findley AS, Monziani A, Richards AL, Rhodes K, Ward MC, Kalita CA, et al. Functional dynamic genetic effects on gene regulation are specific to particular cell types and environmental conditions. Elife. 2021;10. doi:10.7554/eLife.67077

13. Moyerbrailean GA, Richards AL, Kurtz D, Kalita CA, Davis GO, Harvey CT, et al. High-throughput allele-specific expression across 250 environmental conditions. Genome Res. 2016;26: 1627–1638.

14. Knowles DA, Burrows CK, Blischak JD, Patterson KM, Serie DJ, Norton N, et al. Determining the genetic basis of anthracycline-cardiotoxicity by molecular response QTL mapping in induced cardiomyocytes. Elife. 2018;7. doi:10.7554/eLife.33480

15. Gutierrez-Arcelus M, Baglaenko Y, Arora J, Hannes S, Luo Y, Amariuta T, et al. Allele-specific expression changes dynamically during T cell activation in HLA and other autoimmune loci. Nat Genet. 2020; 1–23.

16. Kichaev G, Yang W-Y, Lindstrom S, Hormozdiari F, Eskin E, Price AL, et al. Integrating Functional Data to Prioritize Causal Variants in Statistical Fine-Mapping Studies. PLoS Genet. 2014;10: e1004722-16.

17. Kichaev G, Bhatia G, Loh P-R, Gazal S, Burch K, Freund MK, et al. Leveraging Polygenic Functional Enrichment to Improve GWAS Power. Am J Hum Genet. 2019;104: 65–75.

18. Weissbrod O, Hormozdiari F, Benner C, Cui R, Ulirsch J, Gazal S, et al. Functionally informed fine-mapping and polygenic localization of complex trait heritability. Nat Genet. 2020;52: 1355–1363.

19. Kubota N, Suyama M. Functional variants in hematopoietic transcription factor footprints and their roles in the risk of immune system diseases. bioRxiv. 2021. p. 2021.03.22.436360. doi:10.1101/2021.03.22.436360

20. Chen J, Rozowsky J, Galeev TR, Harmanci A, Kitchen R, Bedford J, et al. A uniform survey of allele-specific binding and expression over 1000-Genomes-Project individuals. Nat Commun. 2016;7: 11101.

21. Tehranchi AK, Myrthil M, Martin T, Hie BL, Golan D, Fraser HB. Pooled ChIP-Seq Links Variation in Transcription Factor Binding to Complex Disease Risk. Cell. 2016;165: 730–741.

22. Abramov S, Boytsov A, Bykova D, Penzar DD, Yevshin I, Kolmykov SK, et al. Landscape of allele-specific transcription factor binding in the human genome. Nat Commun. 2021;12: 2751.

23. Inoue F, Kircher M, Martin B, Cooper GM, Witten DM, McManus MT, et al. A systematic comparison reveals substantial differences in chromosomal versus episomal encoding of enhancer activity. Genome Res. 2017;27: 38–52.

24. Lou H, Yeager M, Li H, Bosquet JG, Hayes RB, Orr N, et al. Fine mapping and functional analysis of a common variant in MSMB on chromosome 10q11.2 associated with prostate cancer susceptibility. Proc Natl Acad Sci U S A. 2009;106: 7933–7938.

25. Meyer KB, O'Reilly M, Michailidou K, Carlebur S, Edwards SL, French JD, et al. Fine-scale mapping of the FGFR2 breast cancer risk locus: putative functional variants differentially bind FOXA1 and E2F1. Am J Hum Genet. 2013;93: 1046–1060.

26. Gupta RM, Hadaya J, Trehan A, Zekavat SM, Roselli C, Klarin D, et al. A Genetic Variant Associated with Five Vascular Diseases Is a Distal Regulator of Endothelin-1 Gene Expression. Cell. 2017;170: 522-533.e15.

27. Zhao Q, Dacre M, Nguyen T, Pjanic M, Liu B, Iyer D, et al. Molecular mechanisms of coronary disease revealed using quantitative trait loci for TCF21 binding, chromatin accessibility, and chromosomal looping. Genome Biol. 2020;21: 135.

28. Waszak SM, Delaneau O, Gschwind AR, Kilpinen H, Raghav SK, Witwicki RM, et al. Population Variation and Genetic Control of Modular Chromatin Architecture in Humans. Cell. 2015;162: 1039–1050.

29. He Y, Chhetri SB, Arvanitis M, Srinivasan K, Aguet F, Ardlie KG, et al. Mechanisms of tissue-specific genetic regulation revealed by latent factors across eQTLs. bioRxiv. 2019. pp. 1–17. Available: http://biorxiv.org/lookup/doi/10.1101/785584

30. Hormozdiari F, Kostem E, Kang EY, Pasaniuc B, Eskin E. Identifying Causal Variants at Loci with Multiple Signals of Association. Genetics. 2014; 1–21.

31. Taylor-Weiner A, Aguet F, Haradhvala NJ, Gosai S, Anand S, Kim J, et al. Scaling computational genomics to millions of individuals with GPUs. Genome Biol. 2019;20: 228.

32. Simon R, Wiegreffe C, Britsch S. Bcl11 Transcription Factors Regulate Cortical Development and Function. Front Mol Neurosci. 2020;13: 51.

33. Akhtar MW, Kim M-S, Adachi M, Morris MJ, Qi X, Richardson JA, et al. In vivo analysis of MEF2 transcription factors in synapse regulation and neuronal survival. PLoS One. 2012;7: e34863.

34. Gregoire FM, Smas CM, Sul HS. Understanding adipocyte differentiation. Physiol Rev. 1998;78: 783–809.

35. Seifert LL, Si C, Saha D, Sadic M, de Vries M, Ballentine S, et al. The ETS transcription factor ELF1 regulates a broadly antiviral program distinct from the type I interferon response. PLoS Pathog. 2019;15: e1007634.

36. Taniguchi T, Ogasawara K, Takaoka A, Tanaka N. IRF Family of Transcription Factors as Regulators of Host Defense. Annu Rev Immunol. 2001;19: 623–655.

37. Hayden MS, Ghosh S. NF-κB in immunobiology. Cell Res. 2011;21: 223–244.

38. Hillmer EJ, Zhang H, Li HS, Watowich SS. STAT3 signaling in immunity. Cytokine Growth Factor Rev. 2016;31: 1–15.

39. Ortiga-Carvalho TM, Sidhaye AR, Wondisford FE. Thyroid hormone receptors and resistance to thyroid hormone disorders. Nat Rev Endocrinol. 2014;10: 582–591.

40. Greenbaum D, Colangelo C, Williams K, Gerstein M. Comparing protein abundance and mRNA expression levels on a genomic scale. Genome Biol. 2003;4: 117.

41. Gry M, Rimini R, Strömberg S, Asplund A, Pontén F, Uhlén M, et al. Correlations between RNA and protein expression profiles in 23 human cell lines. BMC Genomics. 2009;10: 365.

42. Jiang L, Wang M, Lin S, Jian R, Li X, Chan J, et al. A Quantitative Proteome Map of the Human Body. Cell. 2020;183: 269-283.e19.

43. Garcia-Alonso L, Holland CH, Ibrahim MM, Turei D, Saez-Rodriguez J. Benchmark and integration of resources for the estimation of human transcription factor activities. Genome Res. 2019;29: 1363–1375.

44. Abramov S, Boytsov A, Bykova D, Penzar DD, Yevshin I, Kolmykov SK, et al. Landscape of allele-specific transcription factor binding in the human genome. bioRxiv. 2020. p. 2020.10.07.327643. doi:10.1101/2020.10.07.327643

45. Brandt M, Kim-Hellmuth S, Ziosi M, Gokden A, Wolman A, Lam N, et al. An autoimmune disease risk variant has a trans master regulatory effect mediated by IRF1 under immune stimulation. Cold Spring Harbor Laboratory. 2020. p. 2020.02.21.959734. doi:10.1101/2020.02.21.959734

46. McElwee MK, Song MO, Freedman JH. Copper activation of NF-kappaB signaling in HepG2 cells. J Mol Biol. 2009;393: 1013–1021.

47. Hu Frisk JM, Kjellén L, Kaler SG, Pejler G, Öhrvik H. Copper Regulates Maturation and Expression of an MITF:Tryptase Axis in Mast Cells. J Immunol. 2017;199: 4132–4141.

48. Wen X, Pique-Regi R, Luca F. Integrating molecular QTL data into genome-wide genetic association analysis: Probabilistic assessment of enrichment and colocalization. PLoS Genet. 2017;13: e1006646-25.

49. Barbeira AN, Bonazzola R, Gamazon ER, Liang Y, Park Y, Kim-Hellmuth S, et al. Exploiting the GTEx resources to decipher the mechanisms at GWAS loci. Genome Biol. 2021;22: 49.

50. Astle WJ, Elding H, Jiang T, Allen D, Ruklisa D, Mann AL, et al. The Allelic Landscape of Human Blood Cell Trait Variation and Links to Common Complex Disease. Cell. 2016;167: 1415-1429.e19.

51. Georgopoulos K. Haematopoietic cell-fate decisions, chromatin regulation and ikaros. Nat Rev Immunol. 2002;2: 162–174.

52. Ezzat S, Mader R, Fischer S, Yu S, Ackerley C, Asa SL. An essential role for the hematopoietic transcription factor Ikaros in hypothalamic-pituitary-mediated somatic growth. Proc Natl Acad Sci U S A. 2006;103: 2214–2219.

53. Kheradpour P, Kellis M. Systematic discovery and characterization of regulatory motifs in ENCODE TF binding experiments. Nucleic Acids Res. 2014;42: 2976–2987.

54. Kulakovskiy IV, Vorontsov IE, Yevshin IS, Sharipov RN, Fedorova AD, Rumynskiy EI, et al. HOCOMOCO: towards a complete collection of transcription factor binding models for human and mouse via large-scale ChIP-Seq analysis. Nucleic Acids Res. 2018;46: D252–D259.

55. ENCODE Project Consortium, Birney E, Stamatoyannopoulos JA, Dutta A, Guigó R, Gingeras TR, et al. Identification and analysis of functional elements in 1% of the human genome by the ENCODE pilot project. Nature. 2007;447: 799–816.

56. Patsoukis N, Bardhan K, Weaver JD, Sari D, Torres-Gomez A, Li L, et al. The adaptor molecule RIAM integrates signaling events critical for integrin-mediated control of immune function and cancer progression. Sci Signal. 2017;10. doi:10.1126/scisignal.aam8298

57. Lagarrigue F, Kim C, Ginsberg MH. The Rap1-RIAM-talin axis of integrin activation and blood cell function. Blood. 2016;128: 479–487.

58. Lafuente EM, van Puijenbroek AAFL, Krause M, Carman CV, Freeman GJ, Berezovskaya A, et al. RIAM, an Ena/VASP and Profilin ligand, interacts with Rap1-GTP and mediates Rap1-induced adhesion. Dev Cell. 2004;7: 585–595.

59. Lagarrigue F, Vikas Anekal P, Lee H-S, Bachir AI, Ablack JN, Horwitz AF, et al. A RIAM/lamellipodin-talin-integrin complex forms the tip of sticky fingers that guide cell migration. Nat Commun. 2015;6: 8492.

60. Chang C, Adler CE, Krause M, Clark SG, Gertler FB, Tessier-Lavigne M, et al. MIG-10/lamellipodin and AGE-1/PI3K promote axon guidance and outgrowth in response to slit and netrin. Curr Biol. 2006;16: 854–862.

61. Irvine WJ, Wu FCW, Urbaniak SJ, TOOLIS Endocrinology and F. Peripheral blood leucocytes in thyrotoxicosis. Clin Exp Immunol. 1977;27: 216–221.

62. Ahmed SS, Mohammed AA. Effects of thyroid dysfunction on hematological parameters: Case controlled study. Ann West Med Surg. 2020;57: 52–55.

63. Findley AS, Richards AL, Petrini C, Alazizi A, Doman E, Shanku AG, et al. Interpreting Coronary Artery Disease Risk Through Gene-Environment Interactions in Gene Regulation. Genetics. 2019; genetics.302419.2019-12.

64. Knowles DA, Davis JR, Edgington H, Raj A, Favé M-J, Zhu X, et al. Allele-specific expression reveals interactions between genetic variation and environment. Nature Publishing Group. 2017; 1–6.

65. Taylor DL, Knowles DA, Scott LJ, Ramirez AH, Casale FP, Wolford BN, et al. Interactions between genetic variation and cellular environment in skeletal muscle gene expression. PLoS One. 2018;13: e0195788-17.

66. Alvarez MJ, Shen Y, Giorgi FM, Lachmann A, Ding BB, Ye BH, et al. Functional characterization of somatic mutations in cancer using network-based inference of protein activity. Nat Genet. 2016;48: 838–847.

67. Lin Y-C, Boone M, Meuris L, Lemmens I, Van Roy N, Soete A, et al. Genome dynamics of the human embryonic kidney 293 lineage in response to cell biology manipulations. Nat Commun. 2014;5: 4767.

68. Davis JR, Frésard L, Knowles DA, Pala M, Bustamante CD, Battle A, et al. An Efficient Multiple-Testing Adjustment for eQTL Studies that Accounts for Linkage Disequilibrium between Variants. Am J Hum Genet. 2016;98: 216–224.

69. Aran D, Hu Z, Butte AJ. xCell: digitally portraying the tissue cellular heterogeneity landscape. Genome Biol. 2017;18: 220.

70. Mohammadi P, Castel SE, Brown AA, Lappalainen T. Quantifying the regulatory effect size of cis-acting genetic variation using allelic fold change. Genome Res. 2017;27: 1872–1884.

71. Gao X, Starmer J, Martin ER. A multiple testing correction method for genetic association studies using correlated single nucleotide polymorphisms. Genet Epidemiol. 2008;32: 361–369.